JEE Journal of Ecological Engineering

Journal of Ecological Engineering 2022, 23(6), 67–74
https://doi.org/10.12911/22998993/147837
ISSN 2299–8993, License CC-BY 4.0

Received: 2022.03.10
Accepted: 2022.04.12
Published: 2022.04.20

Improving the Performance of Mg/Cr LDH by Forming Metal Oxides Mg/Cr-Ni Using Coprecipitation Method as Adsorbent for Cationic Dyes

Nova Yuliasari[1], Arini Fousty Badri[1], Patimah Mega Syah Bahar Nur Siregar[2], Neza Rahayu Palapa[3], Mardiyanto[4], Risfidian Mohadi[1], Aldes Lesbani[3*]

[1] Graduate School of Faculty Mathematics and Natural Sciences, Sriwijaya University, Palembang, 30139, Indonesia

[2] Magister Programme Graduate School of Mathematics and Natural Sciences, Sriwijaya University, Palembang, 30139, Indonesia

[3] Research Center of Inorganic Materials and Complexes, Faculty of Mathematics and Natural Sciences, Sriwijaya University, Palembang, 30139, Indonesia

[4] Department of Pharmacy, Faculty of Mathematics and Natural Sciences, Sriwijaya University, Palembang, 30662, Indonesia

* Corresponding author's e-mail: aldeslesbani@pps.unsri.ac.id

ABSTRACT

This study aimed to determine the adsorption capacity of rhodamine-B (Rh-B) and methylene blue (MB) on Mg/Cr-Ni adsorbents. The Mg/Cr-Ni adsorbent was synthesized by the coprecipitation method. The results of the characterization of Mg/Cr-Ni using XRD analysis showed the formation of oxides at an angle of 2θ = 31.726°, 33°, and 45.44°. The surface area of Mg/Cr-Ni is 23.139 m^2/g. The adsorption capacity test for Mg/Cr-Ni for Rh-B and MB were 85.470 mg/g and 166.667 mg/g, respectively. The adsorption kinetics model followed the pseudo second order (PSO). The adsorption process is endothermic and occurs spontaneously at any temperature. Mg/Cr-Ni showed stability in the adsorption process of Rh-B and MB for 5 regeneration cycles.

Keywords: adsorption, metal oxide, rhodamine-b, methylene blue, regeneration.

INTRODUCTION

Dyes are some of the materials that are often used in industry. The textile industry is the largest user of dyes, making it the largest contributor to dye waste in waters (Li et al. 2020). The waste comes from the dyeing process in the form of water-soluble dyes. Dyestuff waste generally has non-biodegradable properties, because it contains complex aromatic compounds that are difficult to decompose by microbes (Zheng et al. 2018). In addition, dye waste is harmful to human health and the biota that live around polluted water bodies. Liu & Pan, (2012) stated that generally, these organic compounds are also teratogenic (causing defects in the fetus during pregnancy), carcinogenic (causing cancer) and mutagenic (causing gene mutations) so that they can pose a serious threat to human health. Commonly used hazardous dyes include Rh-B and MB (Shi et al., 2020; Wan Ngah et al., 2011). Excessive entry of Rh-B and MB (Figure 1) into the environment will change the pH of the waters, so that the microorganisms and animals in the aquatic environment will be disturbed. In the human body, the accumulation of these dyes will cause serious impacts, such as poisoning, liver cancer, respiratory tract irritation, skin irritation, and digestive tract irritation (Nkutha, Shooto, and Naidoo 2020; Sagita, Nulandaya, and Kurniawan 2021; Wei et al. 2015). Various methods, such as adsorption, have been developed to

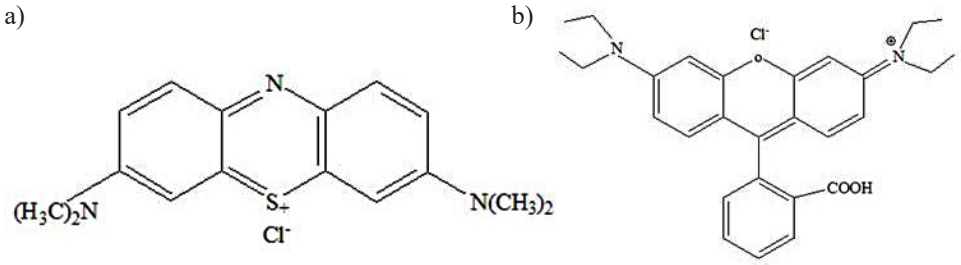

Figure 1. Structure of MB (a) and Rh-B (b)

remove dyes from wastewater. Adsorption is an effective method for treating dyestuffs in wastewater, because the technique is simple, economical and environmentally friendly (Conrad et al. 2016; Xu et al. 2020).

Layered double hydroxide (LDH) is an adsorbent that is widely used in the process of removing pollutants from aqueous solutions, but its direct use is not very effective, due to the small surface area and poor structural stability (Marques et al. 2020). Several methods have been applied to improve the adsorption performance (adsorption capacity, structural stability, and resistance to chemical environment), namely by modifying LDH. Recently, many researchers have focused on adsorption using metal oxide adsorbents such as aluminum oxide, titanium oxide, iron oxide, manganese oxide, zirconium oxide. This is because metal oxides have nano size, large surface area, and exhibit good activity, so that they are effectively used in the process of removing pollutants from aqueous solutions (Taman et al. 2018).

In this study, the adsorption of Rh-B and MB was carried out using the Mg/Cr-Ni metal oxide. The synthesis of metal oxide Mg/Cr-Ni was based on the coprecipitation method. The intercalated Mg/Cr-Ni were characterized using XRD, FTIR, and BET analysis. Then the stability of Mg/Cr-Ni was tested by regeneration studies and continued for the adsorption process, which included the effect of concentration and temperature, as well as the effect of contact time between the adsorbent and the adsorbate used.

MATERIAL AND METHODS

Materials

The materials used included $Mg(NO_3)_2.6H_2O$, $Cr(NO_3)_2.9H_2O$, metal oxides $Ni(NO_3)_2.6H_2O$, distilled water, methylene blue, rhodamine-B, HCl, and NaOH.

Methods

Synthesis of Mg/Cr

In this study, 100 mL $Mg(NO_3)_2.6H_2O$ solution and $Cr(NO_3)_2.9H_2O$ solution with a ratio 3:1 (0.75:0.25). The mixture was adjusted pH to 10 and stirred for 4 hours. The precipitate obtained, filtered, dried and characterized.

Synthesis of Mg/Cr-Ni

In this study, 100 mL of $Mg(NO_3)_2.6H_2O$ 0.75 M and 100 mL of $Cr(NO_3)_2.9H_2O$ 0.25 in a ratio (3:1), were stirred at 80°C and added 2 M NaOH to pH 10. The mixture was added 0.25 mL $Ni(NO_3)_2.6H_2O$ 0.5 M. After forming a precipitate, the gel was heated at 80°C for 24 hours and then baked at 250°C for 6 hours, then characterized.

Adsorption study

Regeneration

In the experiment, 10 mL of methylene blue (100 mg/L) and adsorbent (0.1 g) were added. The mixture was stirred for 2 hours, after 2 hours the filtrate was measured. The adsorbent that has been used in the adsorption process was desorbed using distilled water with an ultrasonic system. The adsorbent was then dried and the same treatment was carried out for the next cycle.

Variation of concentration and temperature

The effect of concentration and temperature on the adsorption of Mg/Cr-Ni was studied by varying the concentration and temperature. A total of 0.025 g Mg/Cr-Ni was added to an Erlenmeyer flask containing 25 mL of methylene blue, stirred for 1 hour. After stirring is complete, the filtrate is measured.

Effect of contact time

The contact time of the adsorbent with the adsorbate was studied by varying the time. The solution (100 mg/L, 25 mL) was added with 0.025 g Mg/Cr-Ni then the mixture was stirred and the filtrate was measured.

Characterization

The adsorbent was characterized using an X-Ray Rigaku Miniflex-600 diffractometer, Shimadzu Prestige-21 FTIR Spectrophotometer, BET Surface Area Analyzer Micrometric ASAP Quantachrome, and UV-Visible Biobase Spectrophotometer BKUV1800PC.

RESULT AND DISSCUSION

The analysis carried out with X-ray diffractograms obtained results in the form of diffraction patterns of Mg/Cr and Mg/Cr-Ni as shown in Figure 2. Figure 2(a) is a diffractogram pattern of layered double hydroxide Mg/Cr where diffraction peaks appear at angles of 2θ = 12.45° and 61.44° which are characteristic of layered double hydroxide materials (Badri, et al., 2021). The research conducted by Badri et al. (2021), MgAl-LDH was impregnated with biochar to manufacture a Mg-Al/Biochar composite. The composite was characterized using powder X-ray diffraction (XRD reported that the diffraction peaks which appeared around the angles of 11° and 60° with high intensity indicated the successful synthesis of layered double hydroxide. The XRD results of Mg/Cr-Ni powder shown in Figure 2(b) show high peaks that appear at angles of 2θ = 31.726°, 33°, and 45.44° which indicate the material is an oxide.

Figure 3 shows that there is stretching vibration of the hydroxyl group (OH) in Mg/Cr and Mg/Cr-Ni which is indicated at a wave number of 3448 cm^{-1}. The spectrum that appears at wave numbers 1643 cm^{-1} and 1627 cm^{-1} is an aromatic C=C group. At wave numbers with a peak range between 594 cm^{-1} to 640 cm^{-1} there is a metallic bond (Mg-O) for Mg/Cr and Mg/Cr-Ni. This corresponds to the characteristic for vibrations lower than 800 cm^{-1} which is known as metallic oxygen bonding in the mixture.

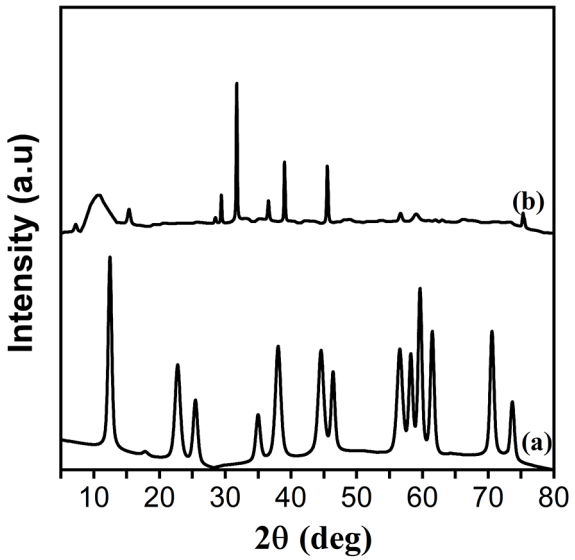

Figure 2. XRD analysis of Mg/Cr (a) and Mg/Cr-Ni (b)

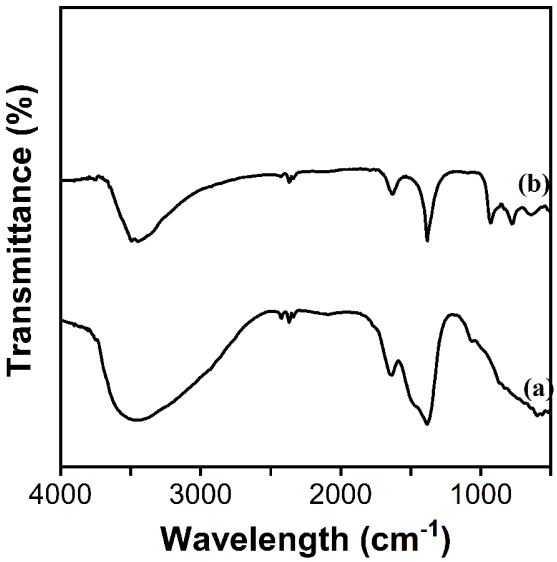

Figure 3. FTIR analysis of Mg/Cr (a) and Mg/Cr-Ni (b)

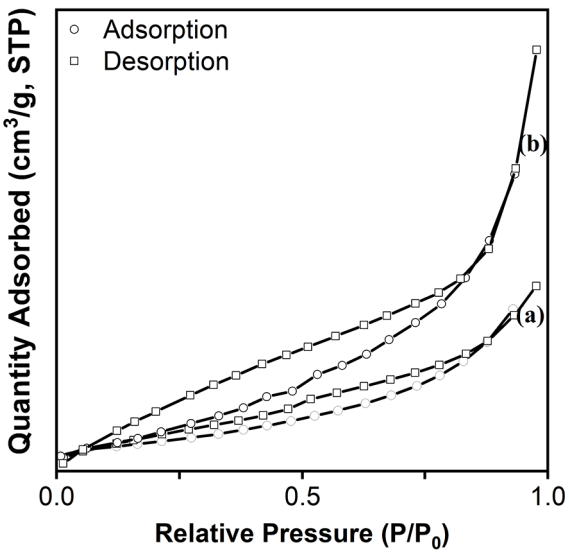

Figure 4. BET profile of Mg/Cr (a) and Mg/Cr-Ni (b)

Table 1. Surface area of material

Material	Surface area (m^2/g)
Mg/Cr	21.511
Mg/Cr-Ni	23.139

The surface area of the material was analyzed using the Brunnaeur Emmet Teller (BET) analysis. Figure 4 shows that the adsorbent follows the type IV isotherm according to the classification by IUPAC (Normah et al. 2021). Type IV isotherm indicates the occurrence of hysteresis phenomena and the formation of layers (Siregar et al. 2022). From the results of the BET analysis shown in Table 1 it can be concluded that the Mg/Cr-Ni made of layered double hydroxide Mg/Cr modified through the co-precipitation method showed that the modified material (Mg/Cr-Ni) produced a larger surface area compared to the modified material base (Mg/Cr). Materials with a larger surface area are used as adsorbents in the adsorption process of MB and Rh-B.

Regeneration is the repeated use of an adsorbent. Regeneration is carried out through desorption first to release the adsorbate that has been adsorbed so that the adsorbent can be reused (Lv et al. 2019). Regeneration is also an alternative to overcome the problems caused by the adsorption process, namely the presence of adsorbent waste which is more dangerous than the adsorbate waste itself. In this research, a regeneration study was conducted to see the ability of the material. The adsorption efficiency of Rh-B and MB using the Mg/Cr-Ni adsorbent for the regeneration process decreased drastically in the 4th and 5th cycles as shown in Figure 5.

Figure 6 shows an increase in the adsorbed concentration as the temperature used increases. This indicates that the temperature affects the rate of adsorption and the equilibrium conditions in the adsorption process (Juleanti et al. 2021). On the basis of Table 2, it is known that equilibrium is reached at a temperature of 60°C with the maximum adsorption capacity of Mg/Cr-Ni of 85.470 mg/g and 166.667 mg/g for Rh-B and MB. This

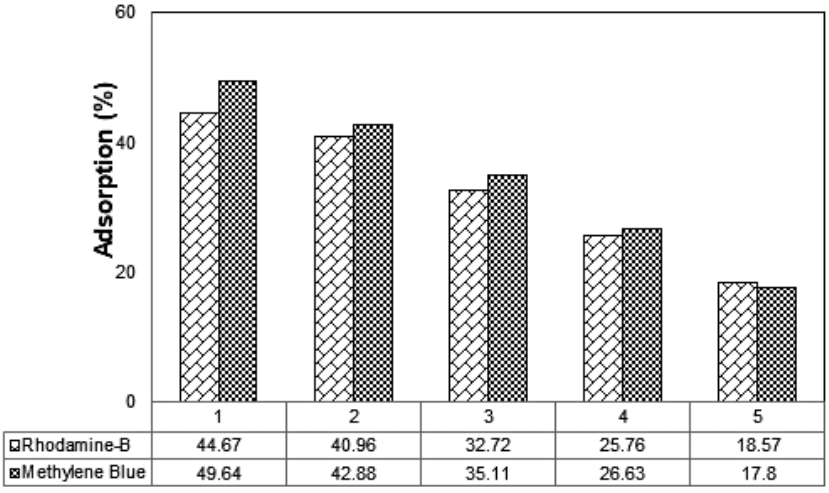

Figure 5. Regeneration of Mg/Cr-Ni

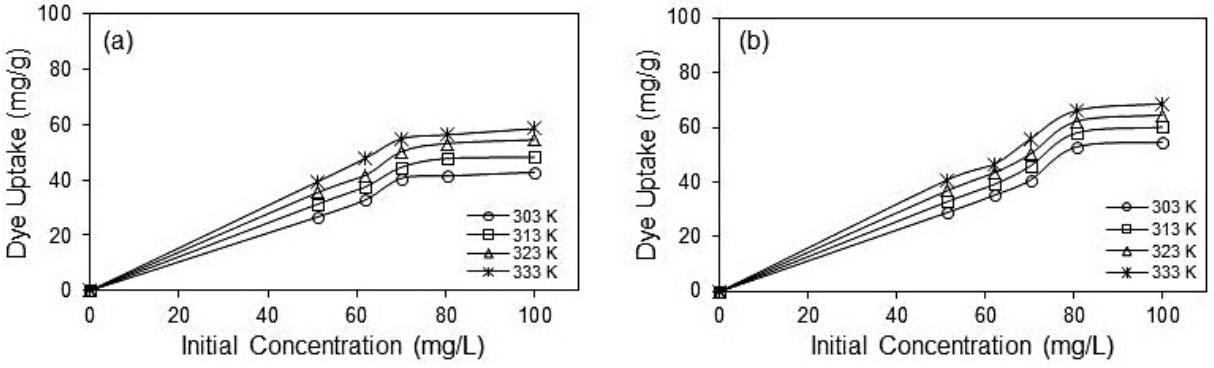

Figure 6. Effect concentration and temperature of Rh-B (a) and MB on adsorption temperature using Mg/Cr-Ni

Table 2. Isotherm adsorption of Mg/Cr-Ni

Dyes	Adsorption Isotherm	Adsorption Constant	T			
			30°C	40°C	50°C	60°C
RhB	Langmuir	Qmax	6.510	13.387	72.993	85.470
		kL	0.048	0.244	0.040	0.097
		R^2	0.972	0.995	0.814	0.936
	Freundlich	*n*	0.964	0.523	1.316	3.142
		kF	1.710	20.54	2.669	17.278
		R^2	0.999	0.986	0.975	0.968
MB	Langmuir	Qmax	44.053	55.249	84.034	166.667
		kL	0.012	0.010	0.016	0.009
		R^2	0.837	0.887	0.95	0.957
	Freundlich	n	0.571	0.578	0.691	0.689
		kF	12.3	8.24	2.309	1.694
		R^2	0.999	0.998	0.999	0.957

indicates that MB is more easily adsorbed than Rh-B, which is characterized by a greater maximum adsorption capacity of MB and a simple molecular structure than Rh-B, as shown in Figure 1.

The solid-liquid phase adsorption usually follows the Langmuir and Freundlich isotherm type (Jain et al., 2016; Zhang et al., 2014). Chemical and physical bonds can occur between the adsorbate molecules and the surface of the adsorbent. The adsorption isotherm model can be determined by looking at the correlation coefficient (R^2) which is closer to 1 (Buaphean, Ketwongsa, and Piyamongkala 2017). On the basis of the comparison of the two types of adsorption isotherms, the linearity of the Freundlich adsorption isotherm is closer to the value of 1, compared to the Langmuir isotherm. Thus, adsorption is physical in nature where heterogeneous adsorbent surfaces have adsorption sites with different bond energies (multilayer) (Nkutha, Shooto, and Naidoo 2020).

Thermodynamic parameters are used for information regarding the direction and energy changes that occur in the adsorption process of Rh-B and MB with Mg/Cr-Ni adsorbents, including changes in enthalpy (ΔH) (Wang, Yan, and Wang 2013), changes in entropy (ΔS) (Patil et al. 2017), and changes in Gibbs free energy (ΔG) (Dotto et al. 2015). The negative value of ΔG indicates that the adsorption process runs spontaneously. A positive value for ΔH indicates that the adsorption reaction is endothermic, while the value of ΔS indicates that the degree of disorder in the adsorption process is small. Table 3 contains the thermodynamic data for the adsorption of Rh-B and MB using Mg/Cr-Ni at temperatures of 30, 40, 50, and 60°C.

On the basis of the results of the study shown in Figure 7, the equilibrium adsorption of Rh-B and MB (qe) by Mg/Cr-Ni occurred at 150 minutes. After the equilibrium was reached, with increasing time there was still an increase in MB adsorption but it was not significant, so it was concluded that the time adsorption equilibrium was at 150 minutes.

Adsorption kinetics is one aspect that is often studied to evaluate the characteristics of the

Table 3. Thermodynamic adsorption of Mg/Cr-Ni

Dyes	*T* (K)	Q_e (mg/g)	Δ*H* (kJ/mol)	Δ*S* (J/mol K)	ΔG (kJ/mol)
Rh-B	303	26.670	23.942	0.077	0.609
	313	31.288			-0.161
	323	35.450			-0.931
	333	39.384			-1.701
MB	303	28.884	22.571	0.074	0.294
	313	32.826			-0.441
	323	36.828			-1.177
	333	40.770			-1.912

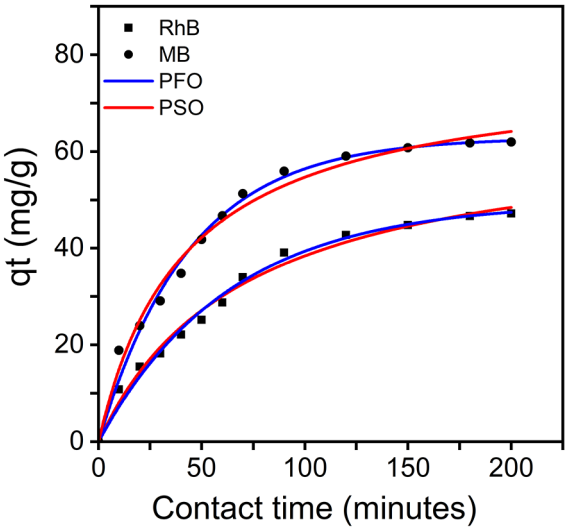

Figure 7. Adsorption contact time of Mg/Cr-Ni

adsorbent used. Kinetics describes the rate of adsorbate adsorption on changes in the contact time of a reaction. The kinetic model that is often encountered is PFO which describes a reversible equilibrium between the liquid phase (adsorbate) and the solid phase (adsorbent) (Wijaya et al. 2021). The second kinetic model is PSO explaining that the rate limiting step of the adsorption considered is chemical adsorption through various mechanisms, such as electrostatic interactions, or complex formation (Amin, Alazba, and Shafiq 2020). The data Table 4 show that the appropriate adsorption kinetics in this study followed PSO. This can be indicated through the value of the linear regression coefficient (R^2) in the PSO equation which is close to the value 1, namely 0.9823 and 0.9913 for Rh-B and MB.

CONCLUSIONS

On the basis of the research that has been conducted, it can be concluded that Mg/Cr-Ni is an adsorbent that can be used repeatedly for 5 cycles seen from the regeneration results in the adsorption process of Rh-B and MB. The maximum adsorption capacity occurred at a temperature of 60°C, namely Rh-B of 85.470 mg/g and MB of 166.667 mg/g. The adsorption isotherms of Rh-B and MB followed the Freundlich isotherm equation with the R^2 values of 0.9677 and 0.9575. The adsorption kinetics model followed

Table 4. Kinetic parameter

Dyes	Initial concentration (mg/L)	$Qe_{exp.}$ (mg/g)	PFO			PSO		
			$Qe_{Calc.}$ (mg/g)	R^2	$k1$	$Qe_{Calc.}$ (mg/g)	R^2	$k2$
RhB	101.180	47.206	57.730	0.969	0.023	63.694	0.982	0.0002
MB	101.180	61.977	75.370	0.981	0.029	75.758	0.991	0.0003

Table 5. Adsorption of MB and Rh-B using several adsorbents

Adsorbent	Dyes	Adsorption capacity (mg/g)	References
Iron Oxide Magnetic Nanoparticles	Methylene Blue	37.45	(Razali et al., 2020)
Fe_3O_4/ZrO_2		90.9	(Kristianto & Saleh, 2018)
Fe_3O_4/ZrO_2/NGP		125	(Kristianto & Saleh, 2018)
Hydroxyapatite-Fe_3O_4 composite		12.434	(Abidin et al., 2019)
Reduced graphene oxide		107.53	(Arias et al., 2020)
CuO		28.66	(Al-Aoh et al., 2019)
CuO-Al_2O_3 nano-materials		97.04	(Zhang et al., 2014)
Fe_3O_4/NiO		40.1	(Razali et al., 2020)
Mg/Cr-Ni		166.667	This Research
Magnetic nanocomposite	Rhodamine-B	29.48	(Singh et al., 2010)
RGO-Ni nanocomposite		65.31	(Jinendra et al., 2021)
Ligno sulfonate Fe_3O_4		22.47	(Geng et al., 2019)
Bi_2O_3-bentonite nanocomposite		31.25	(Patil et al., 2015)
SDS-modified α-Al_2O_3		52	(Doan et al., 2020)
Paper industry		6.711	(Thakur & Kaur, 2017)
NiO/SiO_2 nanocomposites		68	(Rubab et al., 2021)
Mg/Cr-Ni		85.470	This research

pseudo second order (PSO). Adsorption in this study includes physical adsorption with adsorption heat capacity (ΔH) of 23.942 kJ/mol for Rh-B and 22.571 kJ/mol for MB is endothermic, and occurs spontaneously.

Acknowledgements

All authors express special thanks to the Laboratory of Inorganic Materials and Complexes of the Faculty of Mathematics and Natural Sciences, Sriwijaya University for support of this research. Thanks to Ministry of Education, Culture, Research and Technology through by Hibah Disertasi Doktor 2021-2022 as additional output based research.

REFERENCES

1. Amin M.T., Alazba A.A., Shafiq M. 2020. LDH of NiZnFe and Its Composites with Carbon Nanotubes and Data-Palm Biochar with Efficient Adsorption Capacity for RB5 Dye from Aqueous Solutions: Isotherm, Kinetic, and Thermodynamics Studies. Current Applied Physics, 1–11.
2. Badri, Fousty A., Siregar P.M.S.B.N., et al. 2021. Mg-Al/Biochar Composite with Stable Structure for Malachite Green Adsorption from Aqueous Solutions." Bulletin of Chemical Reaction Engineering & Catalysis, 16(1), 149–160.
3. Badri F.A., Palapa N.R., et al. 2021. Mg-Cr Layered Double Hydroxide with Intercalated Oxalic Anion for Removal Cationic Dyes Rhodamine B and Methylene Blue. Journal of Environmental Treatment Techniques, 9(2), 383–391.
4. Buaphean T., Ketwongsa T., Piyamongkala K. 2017. Coagulation of Chitosan Solution in Commercial Detergent as Adsorbent for Sorption Methylene Blue Dye. Solid State Phenomena, 266, 122–127.
5. Conrad Enenebeaku K. et al. 2016. Adsorption of Congo Red Dye from Aqueous Solution Using Agricultural Waste. IOSR Journal of Applied Chemistry (IOSR-JAC), 9(9), 39–51.
6. Dotto G.L. et al. 2015. Adsorption of Methylene Blue by Ultrasonic Surface Modified Chitin. Journal of Colloid and Interface Science, 446, 133–140.
7. Jain N., Dwivedi M.K., Waskle A. 2016. Adsorption of Methylene Blue Dye from Industrial Effluents Using Coal Fly Ash. International Journal of Advanced Engineering Research and Science (IJAERS), 3(4), 9–16.
8. Juleanti, Novie et al. 2021. The Capability of Biochar-Based CaAl and MgAl Composite Materials as Adsorbent for Removal Cr (VI) in Aqueous Solution. Science and Technology Indonesia, 6(3), 156–165.
9. Li Z. et al. 2020. Adsorption of Congo Red and Methylene Blue Dyes on an Ashitaba Waste and a Walnut Shell-Based Activated Carbon from Aqueous Solutions : Experiments, Characterization and Physical Interpretations. Chemical Engineering Journal, 388(January), 124263. https://doi.org/10.1016/j.cej.2020.124263.
10. Liu Q., Pan C. 2012. A Novel Route to Treat Wastewater Containing Cationic Dyes. Taylor & Francis, 47(4), 630–635.
11. Lv X, et al. 2019. Nanoscale Zero Valent Iron Supported on MgAl-LDH-Decorated Reduced Graphene Oxide: Enhanced Performance in Cr(VI) Removal, Mechanism and Regeneration. Journal of Hazardous Materials, 373(December 2018), 176–186. https://doi.org/10.1016/j.jhazmat.2019.03.091
12. Marques B.S. et al. 2020. Ca–Al, Ni–Al and Zn–Al LDH Powders as Efficient Materials to Treat Synthetic Effluents Containing o-Nitrophenol. Journal of Alloys and Compounds, 838(2020), 155628.
13. Nkutha S.C., Shooto N.D., Naidoo E.B. 2020. Adsorption Studies of Methylene Blue and Lead Ions from Aqueous Solution by Using Mesoporous Coral Limestones. South African Journal of Chemical Engineering, 34, 151–157.
14. Normah et al. 2021. The Ability of Composite Ni/Al-Carbon Based Material toward Readsorption of Iron(II) in Aqueous Solution. Science and Technology Indonesia, 6(3), 156–165.
15. Patil M.A., Shinde J.K., Jadhav A.L., Deshpande S.R. 2017. Adsorption of Methylene Blue in Waste Water by Low Cost Adsorbent Rice Husk. International Journal of Engineering Research and Technology, 10(1), 246–252.
16. Sagita, Primi C., Nulandaya L., Kurniawan Y.S. 2021. Efficient and Low-Cost Removal of Methylene Blue Using Activated Natural Kaolinite Material. Journal of Multidisciplinary Applied Natural Science, 1(2), 69–77.
17. Shi Z. et al. 2020. Removal of Methylene Blue from Aqueous Solution Using Mg-Fe, Zn-Fe, Mn-Fe Layered Double Hydroxide. Water Science and Technology, 81(12), 2522–2532.
18. Siregar P.M.S.B.N. et al. 2022. Layered Double Hydroxide/C (C=Humic Acid;Hydrochar) As Adsorbents of Cr(VI) Patimah. Science and Technology Indonesia, 7(1), 41–48.
19. Taman R., Ossman M.E., Mansour M.S., Farag A. 2018. Metal Oxide Nano-Particles as an Adsorbent for Removal of Heavy Metals. Advanced Chemical Engineering, 5(3), 1–8.

20. Wan Ngah W.S., Teong L.C., Hanafiah M.A.K.M. 2011. Adsorption of Dyes and Heavy Metal Ions by Chitosan Composites: A Review. Carbohydrate Polymers, 83(4), 1446–1456.
21. Wang P., Yan T., Wang L. 2013. Removal of Congo Red from Aqueous Solution Using Magnetic Chitosan Composite Microparticles. BioResources, 8(4), 6026–6043.
22. Wei W. et al. 2015. Fast Removal of Methylene Blue from Aqueous Solution by Adsorption Onto Poorly Crystalline Hydroxyapatite Nanoparticles. Digest Journal of Nanomaterials and Biostructures, 10(4), 1343–1363.
23. Wijaya A. et al. 2021. Innovative Modified of Cu-Al / C (C = Biochar, Graphite) Composites for Removal of Procion Red from Aqueous Solution, 6(4), 228–234.
24. Xu H., Zhang P., Zhou S.Y., Jia Q. 2020. Fullerene Functionalized Magnetic Molecularly Imprinted Polymer: Synthesis, Characterization and Application for Efficient Adsorption of Methylene Blue. Chinese Journal of Analytical Chemistry, 48(9), e20107–e20113. http://dx.doi.org/10.1016/S1872-2040(20)60045-7
25. Zhang Y. et al. 2014. Biosorption of Fe(II) and Mn(II) Ions from Aqueous Solution by Rice Husk Ash. BioMed Research International, 2014, 1–10.
26. Zheng X. et al. 2018. Efficient Removal of Anionic Dye (Congo Red) by Dialdehyde Microfibrillated Cellulose/Chitosan Composite Film with Significantly Improved Stability in Dye Solution. International Journal of Biological Macromolecules, 107, 283–289.